2015

Evaluating the healing potential of PTH on femoral shaft fractures in B6, C3, and AJ mice

BOSTON UNIVERSITY

SCHOOL OF MEDICINE

Thesis

EVALUATING THE HEALING POTENTIAL OF PTH ON FEMORAL SHAFT FRACTURES IN B6, C3, AND AJ MICE

by

PETER C. FOSTER

B.S., James Madison University, 2012

Submitted in partial fulfillment of the

requirements for the degree of

Master of Science

2015

Approved by

First Reader

Louis Gerstenfeld, Ph.D.
Professor, Department of Biochemistry and Orthopedic Surgery

Second Reader

Margaret Cooke, M.D.
PGY3 Orthopaedic Surgery, Boston Medical Center

EVALUATING THE HEALING POTENTIAL OF PTH ON FEMORAL SHAFT FRACTURES IN B6, C3, AND AJ MICE

PETER C. FOSTER

ABSTRACT

Parathyroid hormone is a vital mediator of bone metabolism and studies have shown that exogenous treatment can enhance the fracture repair process in murine models. Bone remodeling is a complex process that necessitates multiple molecular and cellular interactions that are affected by genetic variations. These differences contribute to both histological and whole organ level differences of fracture healing. This study was performed to determine the effect of genetic variability of fracture healing in mice treated with parathyroid hormone during two time windows. The first window was the first 14-day period post fracture associated with chondrogensis and the second was the day 15 to day 28 post fracture, which is associated with osteogenesis. Three inbred strains of mice A/J (AJ), C57BL/6J (B6), and C3H/HeJ (C3) that have material and structural differences in bone quality were given femoral shaft fractures and healing was evaluated at different time points post fracture using quantitative real-time polymerase chain reaction (qRT-PCR) and qualitative radiographic analysis. Chondrogenic genes Sox9, ColIIa, aggrecan, and ColXa and osteogenic genes ostrix, osteocalcin, BSP, and DMP1 were examined. The temporal analysis of mRNA expression revealed that PTH treatment given in the first 14 days post fracture enhanced osteogenic and chondrogenic expression in B6 mice, but hindered expression in AJ mice. Treatment with PTH from post fracture day 14 to day 28 greatly affected the osteogenic expression of B6 mice, but had little affect on other

animals. Radiographic analysis showed that each strain presents callus formation at approximately day 7 and reaches maximum size at day 21 post fracture. Additionally B6 mice appear with the largest callus and AJ the smallest. Taken together, these results are consistent with past studies in showing that different strains of mice express a unique temporal and mRNA expression pattern of chondrogenic and osteogenic differentiation. Furthermore, these variations affect the biomechanical properties of the fracture callus during bone remodeling.

TABLE OF CONTENTS

LIST OF FIGURES

LIST OF ABBREVIATIONS

AAALAC ..... American Association for the Accreditation of Laboratory Animal Care

Acan ..... Aggrecan

AJ ..... A/J

B6 ..... C57BL/6J

BMD ..... Bone Mineral Density

COLIIa1 ..... Collagen Type II alpha 1

COLX10a1 ..... Collagen Type X alpha 1

C3 ..... C3H/HeJ

cDNA ..... complementary deoxyribonucleic acid

DMP1 ..... Dentin Matrix Acidic Phosphoprotein 1

DNA ..... deoxyribonucleic acid

IACUC ..... Institutional Animal Care and Use Committee

LASC ..... Laboratory Animal Sciences Center

µg ..... micro-gram

µL ..... micro-liter

mRNA ..... messenger ribonucleic acid

PCR ..... polymerase chain reaction

PTH ..... parathyroid hormone

RANK ..... Receptor Activator of Nuclear Factor kappa-B

RANKL ..... Receptor Activator of Nuclear Factor kappa-B Ligand

RT-qPCR ..... real time qualitative polymerase reaction

RNase ..... ribonuclease

RNA ..... ribonucleic acid

SOX9 ..... SRY (Sex determining region Y)-box 9

INTRODUCTION

Fracture healing is a complex process that involves cell and tissue regeneration and remodeling. In addition, many signaling pathways in cartilage, bone, and vasculature have been implicated in fracture healing (Karsenty, 2008). The majority of fractures heals without complication, however, approximately 5 to 10% of fractures in the United States are complicated by malunion or nonunion (Einhorn, 1995). Parathyroid hormone (PTH) has been extensively studied in animal fracture models and is a well-documented mediator of bone metabolism. PTH has been shown to improve bone remodeling and increased rates of callus formation in animal models (Della Rocca, Crist, Murtha, 2010). However, little is know about the effect of PTH and genetic variability on gene expression in murine fracture models. The aim of this study was to explore the effect of PTH and genetic variability on the mRNA expression of osteogenic and chondrogenic genes in Femoral shaft fractures.

Fracture Repair and Bone Remodeling

Fracture repair begins by a recapitulation of molecular and cellular events that occurred during embryonic endochondral bone formation (Gerstenfeld, Cullinane, Barnes, Graves, & Einhorn, 2003). Figure 1 diagrams the bone marrow, cortical and periosteal interaction at the fracture site.

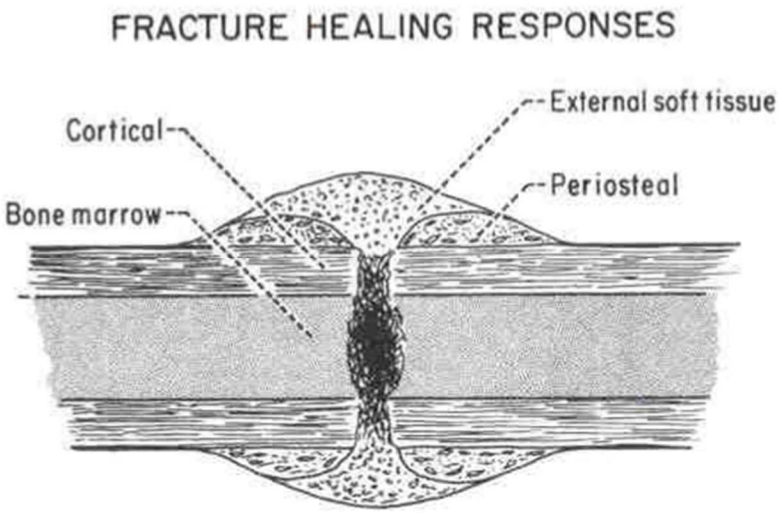

Figure 1. Important sites in fraction healing. Figure taken from Einhorn, 1995.

Inflammation is the first response to a fracture injury. This occurs in the bone marrow, where a blood clot forms in reaction to the injury to the blood vessels in the surrounding area. A majority of the blood vessels in and immediately surrounding the injured area die

and are replaced with cytokine-releasing cells such as with macrophages, neutrophils and platelets within 24 hours (Strohbach, Strong, Rundle, 2011). This leads to the recruitment, infiltration, and proliferation of fibroblasts and skeletogenic stem cells into the periosteum and the formation of granulation tissue around the fracture site.

The recruitment of both osteoprogenitor cells and mesenchymal stem cells into adjacent areas to the fracture site initiate intramembranous ossification and endochondral bone formation (Einhorn, 1998). Both processes work together to promote fracture healing (Gerstenfeld et al., 2006). Intramembranous ossification occurs within a few days post fracture, as seen in Figure 2, where the mesenchymal cells differentiate directly into osteoblasts without a cartilage intermediate mainly at proximal and distal sites to the fracture line (Gerstenfeld et al., 2006).

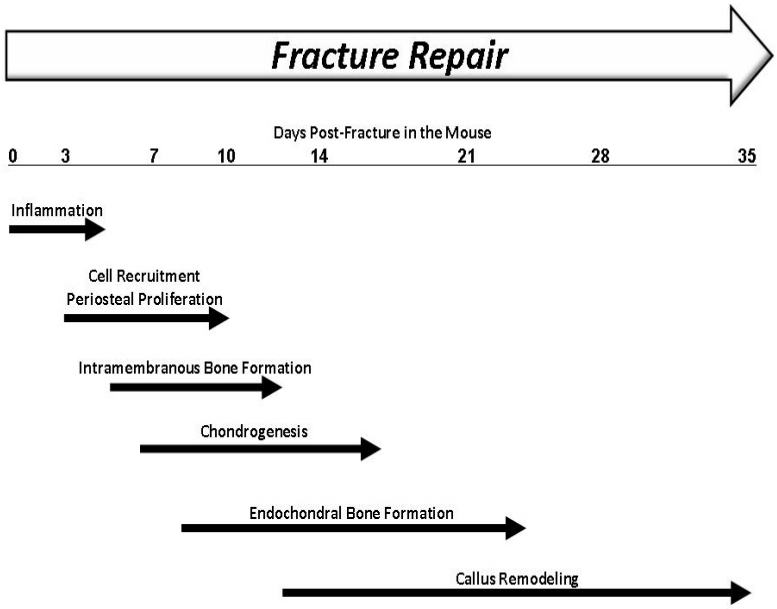

Figure 2. Fracture repair timeline in mice. Figure taken from Strohbach, 2011.

Initially the fracture site is relatively avascular thus inducing chondrogenesis. However, as angiogenesis occurs it becomes a vital component to healing and induces osteogenesis on the periosteal surface as seen in Figure 3. The timing of endochondral bone formation is dependent of the location and severity of the fracture and the relative stability of the bone and which lasts approximately two weeks within mice. Endochondral bone formation is characterized by the development of cartilage scaffolding or callus, which eventually calcifies and is later replaced by lamellar bone (Ross & Pawlina, 2010).

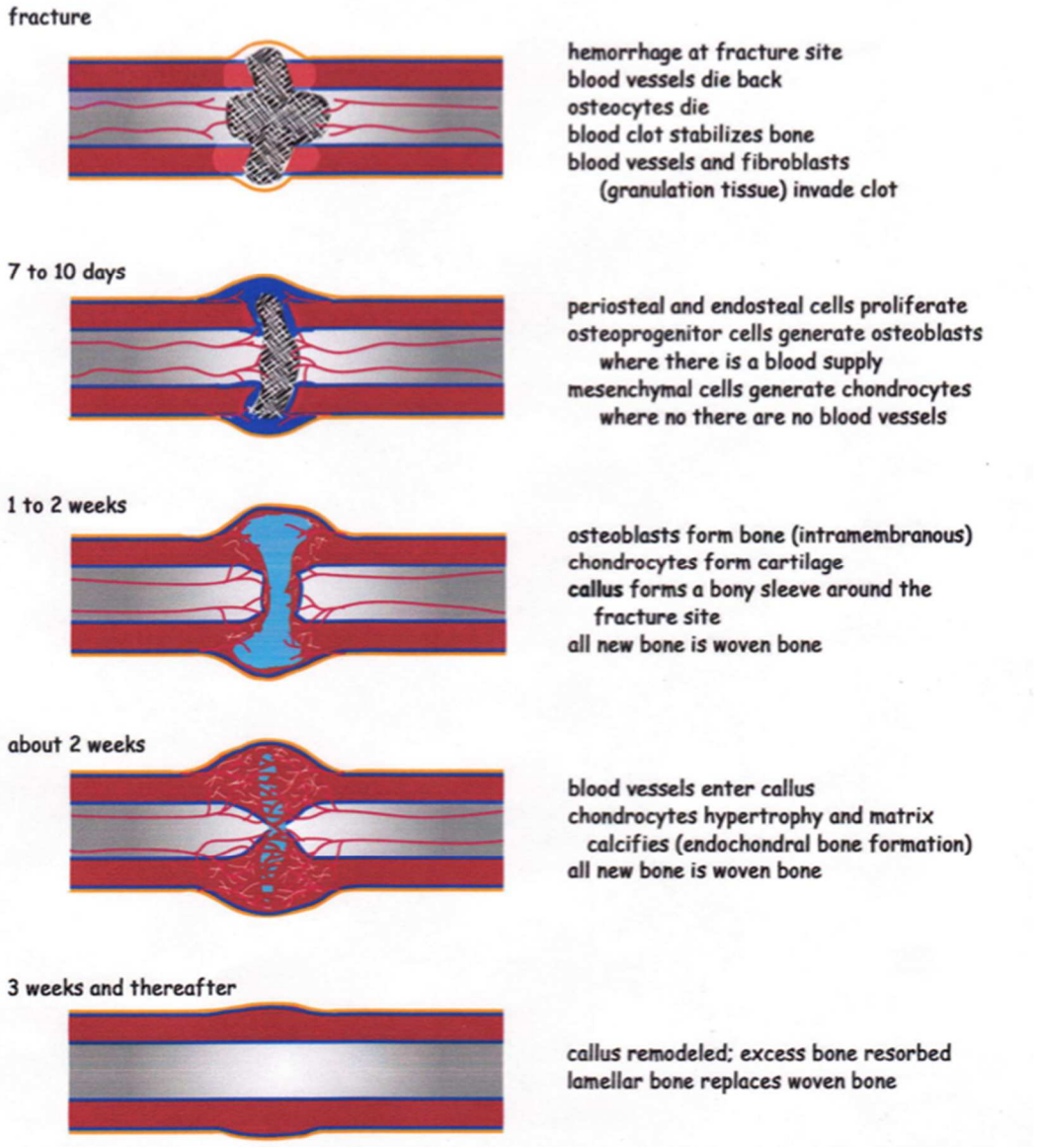

Figure 3. Normal Timeline Associated with Fracture Healing. Major steps involved in fracture healing are listed in the right column with the associated timeframe and illustration in the left column. Figure taken from Vaughn, 2008.

This scaffolding is made up of chondrocytes, which act to stabilize the segmented bone, and are derived from differentiated mesenchymal cells in areas lacking adequate blood supply (Gerstenfeld et al., 2003). Following the formation of the callus and recruitment of blood vessels, the osteoblasts will begin to produce new bone. This leads to resorption of the mineralized cartilage and the transition from woven to lamellar bone. A histological representation of fracture repair is presented in Figure 4.

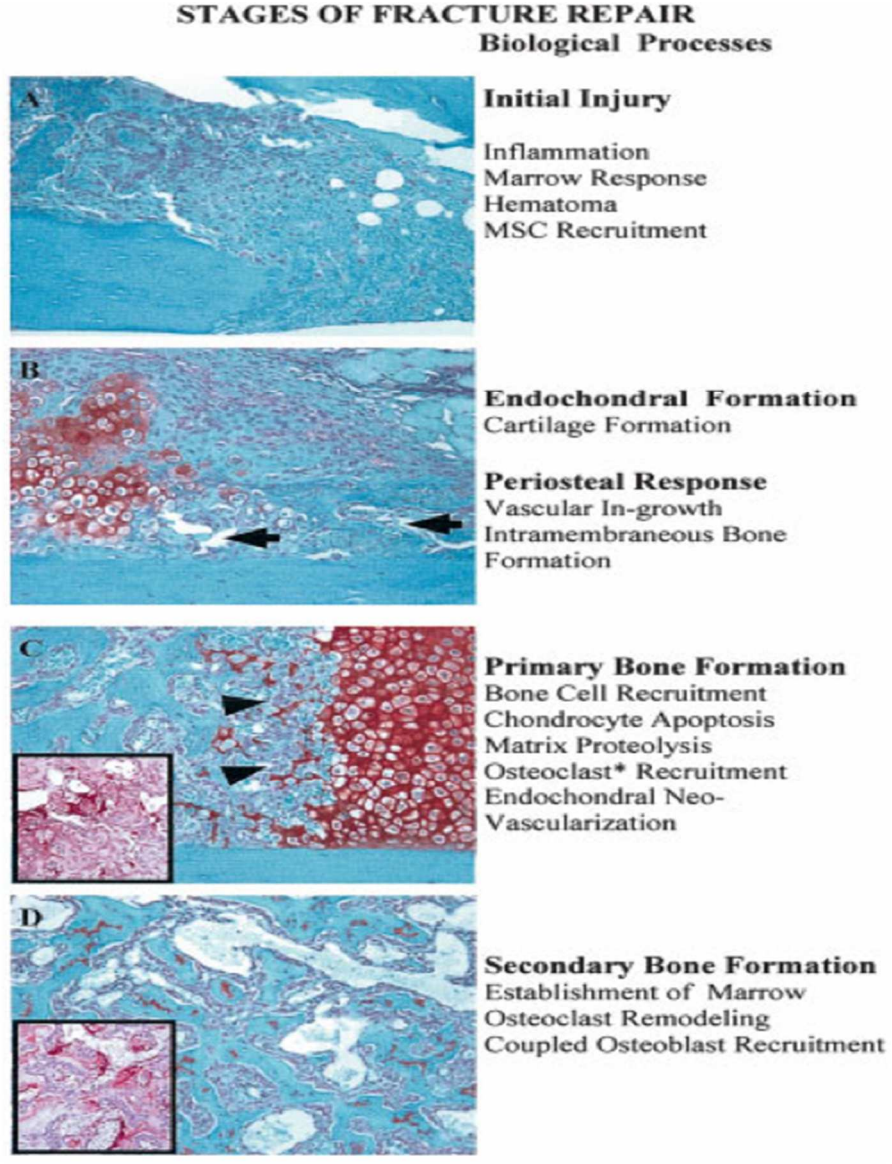

Figure 4. Histology Overview of Fracture Healing. Slides stained with Safarnin O and fast green show sagittal plane of mouse tibia fracture in transverse plane at magnification 200x, Figure taken from Gerstenfeld et al., 2006.

The Role of Parathyroid Hormone (PTH) in Osteogenesis

Parathyroid hormone is an 84-amino acid peptide released by chief cells at the parathyroid glands. Endogenous PTH acts in an endocrine fashion to maintain extracellular calcium levels by triggering osteoclastic bone resorption, gastrointestinal calcium absorption, and renal calcium and phosphate reabsorption (Ellegaard, Jorgensen, Schwartz, 2010). In the bone PTH binding stimulates osteoblastic activity to increase the expression of RANKL and inhibit the expression of osteoprotegerin (OPG) (Pool & Reeve, 2005). OPG binds to RANKL and blocks its interaction with RANK, RANKL's receptor. Binding of RANKL to RANK initiates the formations of new osteoclasts, thereby enhancing bone resorption. Interestingly it has been shown in osteoporotic patients that daily subcutaneous injection of PTH stimulates bone formation and bone mineral density (Neer et al., 2001).

Genetic Variability in Fracture Repair

Twin studies estimate that approximately 70% of variability in adult bone density relate to polygenetic networks (Beamer et al., 1996). Considering the recognized biological diversity in bone quality in genetically diverse individuals, the complex role that these differences display in bone repair is not well understood. It is thus necessary to discover the role that polygenetic networks carry out and how it affects various signal pathways that control fracture repair. It has been suggested that genetic factors may be implicated in impaired fracture healing (Dimitriou, Carr, West, Markham & Giannoudis, 2011). Previous studies have shown that osteogenic and chondrogenic mRNA expression varies between different genetic strains of mice C57BL/6J (B6), A/J (AJ), and C3H/HeJ (C3). More specifically, B6 mice were shown to have a faster progression of endochondral bone formation compared to the C3 and AJ strains (Jepsen et al., 2008). Therefore, due to the genetic variability in bone deposition and repair, additionally studies are needed to clarify the link between genetic variations and fracture healing.

Objectives

Previous studies have shown that PTH enhances fracture healing; however the molecular mechanisms behind these effects and its relation to genetic variance are unclear. Therefore the aim of this study is elucidate this relationship. The hypothesis of this study was that genetic variation would affect fracture healing in mice treated with PTH. This hypothesis was tested by comparing gene expression and callus appearance in A/J (AJ), C3H/HeK (C3), and C57BL/6J (B6) mice. Specifically, mRNA profiles for both osteogenic and chondrogenic genes at various time points during bone remodeling were used to examine temporal differences in gene expression during the fracture healing process. The effect of PTH treatment on fracture healing was evaluated in two groups: One group was treated with PTH for days 1-14 post fracture, and a second group was treated with PTH days 15-28 post fracture. The purpose of this was to determine when in the temporal progression during fracture repair process does PTH particularly effect regulation of known osteogenic and chondrogenic genes.

METHODS

Experimental Design

This study was carried out in accordance with the Institutional Animal Care and Use Committee (IACUC) approved at Boston University School of Medicine (BUSM) and the Federal and United States Department of Agriculture (USDA) guidelines. A total of 288 inbred mice were used for this study; with 96 of each of the three strains C57BL/6J (B6), A/J (AJ), C3H/HeJ (C3). These strains are known to exhibit varying rates of fracture healing time (Jepsen et al., 2008). Male mice were used exclusively in this study to eliminate possible confounding measures that are associated with the role of estrogen in bone metabolism and sexual dimorphism in skeletal structure (Sims et al., 2002). These animals were obtained at approximately 8 to 10 weeks of age from Jackson Laboratories located in Bar Harbor, Maine and housed at the Laboratory Animal Sciences Center (LASC) located on the BUSM campus for the duration of the study. The LASC is accredited by the American Association for the Accreditation of Laboratory Animal Care

(AAALAC). All animals were weighed at time of fracture with weights ranging from 16-26g for AJ, 20-28g for B6, and 18-28 for C3. These weights were subsequently monitored until harvest to assure no mouse exhibited greater than a 20% post surgical reduction in weight

Fracture Procedure

All fracture procedures were carried out within a defined procedure room within the LASC space. Enrolled mice were anesthetized with 5% isoflourane and oxygen via a nose cone and maintained on 1-3% isoflurance for the duration of the procedure. The medial aspect of the right hindlimb was shaved with an electric shaver. Subcutaneous injections of 0.1 ml of 0.5 mg/kg of Buprenex® (buprenorphine) was delivered for post-operative pain management and a dose of 0.01 ml of 2.5 mg/kg Baytril® was administered prophylactically to reduce the risk of infection. The surgical area was aseptically prepared with Betadine® (povidone-iodine).

A small midline skin incision was made over the anterior aspect of the knee; a deep incision medial to the patella was used to expose the distal femur. The patella and patellar ligament were retracted laterally to expose the condylar surface of the femur and a 25G spinal needle was inserted into the medullary canal of the femur until it contacted the proximal physis, in order to stabilize the femur post fracture. Any excess or exposed needle was clipped. The skin incision was then approximated with a 5.0 nylon simple interrupted suture. While anesthetized, the mouse was placed in a supine position with the right leg pulled taught and right femur positioned on a mount underneath a modified fracture apparatus with a blunt blade that was used to generate the Femoral shaft fractures (Marturano et al., 2008). The fracture apparatus releases a weight from a set height to generate the force to create the fracture (Figure 5). The height of the weight was adjusted for size and girth of the animal to create a transverse mid-shaft femur fracture.

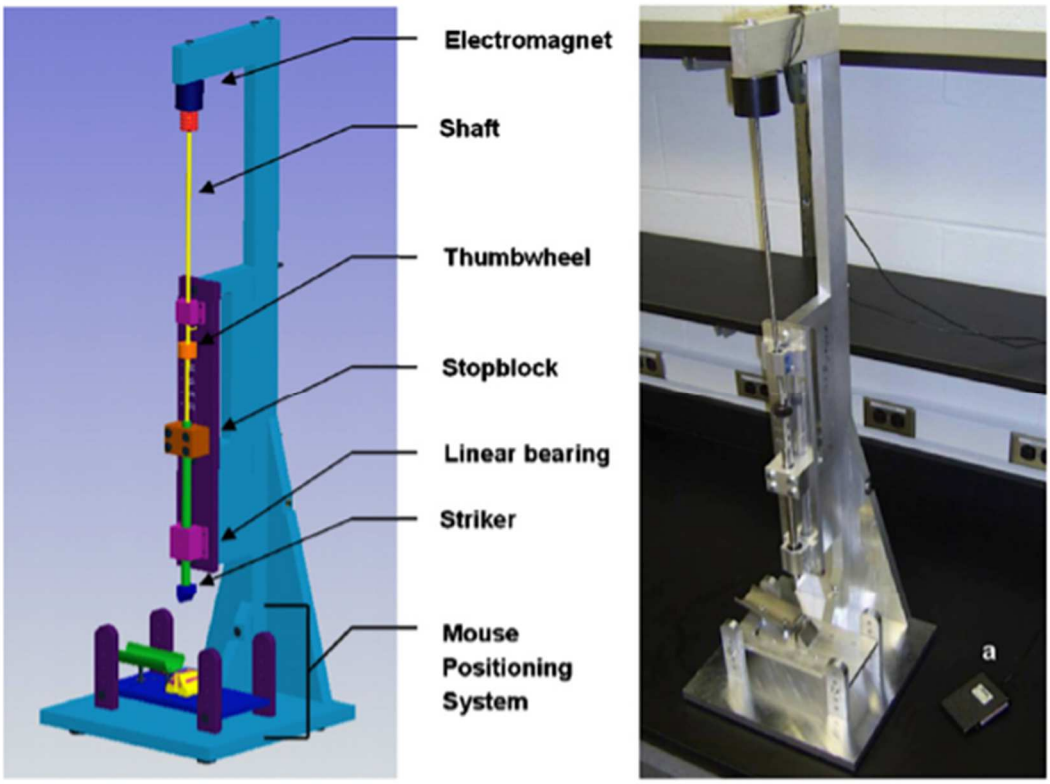

Figure 5. Fracture apparatus. Image on the left is a computer rendering of the fracture apparatus with labeled components used in this study. Image on the right is the actual fracture apparatus, with foot pedal labled "a." (Figure taken from Marturano et al., 2008).

Initial assessment of the fracture was made by gentle palpation. A dental X-ray unit (Gendex, Inc.) at 60kV for 0.16 seconds using Kodak Ultra Speed DF-50 Size 4 film was used to confirm the fracture. These films were manually developed and examined. Femur with proximal, distal, or comminuted fractures or those with severe pin angulations were excluded from the study.

Post-Operative Treatment

Mice were closely monitored post procedure until the animals regained consciousness and were ambulatory. On postoperative day 1, each animal was given injections of buprenorphine at 0.1 mg/kg as an analgesic. Mice were examined daily for signs of hydration, pain, nerve damage, pin retraction, and any signs of failure to recover from injury until tissue harvest.

Parathyroid Hormone Treatment

Two groups of parathyroid hormone (PTH) treatment – group 1 and group 2. Group 1 received daily, subcutaneous injections of 1 cc 0.75 μg human PTH (1-34, BACHEM ®) mixed with sterile H_2O beginning on day 1 post fracture continuing until harvest or day 14 post fracture, whichever came first. The second treatment group

received injections from day 15 until harvest or day 28 post fracture, whichever came first. PTH was stored at –80 C.

Femur Harvest

Fractured femurs were harvested on postoperative day 1, 3, 5, 7, 10, 14, 18, 21, 28, and 35. Right hind limb femurs on non-fractured mice were harvested and used for day 0 controls. Euthanasia was accomplished by carbon dioxide inhalation. Animals were placed individually a plastic chamber and closed with a stainless steel lid and attached flow meter. Carbon dioxide flow was set at a rate of 20% air displacement per minute. Terminal cardiac bleeding after carbon dioxide asphyxiation was also performed and the blood was placed on ice and centrifuged for 10 minutes at 14000 rpm. A thoracotomy was performed and the blood plasma was extracted and frozen at -80°C for each animal for further studies. X-rays were taken immediately following cervical dislocation using a Faxitron MX-20 Specimen Radiography System for a time of 40

seconds at 30kV and a distance of approximately 13 cm. Kodak BioMax XAR Scientific Imaging Film was used.

To harvest femur, an incision was made on the posterior side of right femur and the skin was removed from the muscle. The right leg was then amputated at the hip joint and the muscle and tissue carefully pulled away from femur as to not harm the fracture callus. A number 15 blade was used to cut separate the femur from the tibia and fibula. The spinal needle was pulled from the center canal of the femur with a needle driver. The resulting fracture callus was then isolated by removing both the distal and proximal ends of the femur and placed into an RNA-ase free 2 mL Eppendorf tube. These tubes were immediately placed into liquid nitrogen and stored at -80°C until the time of RNA extraction. The contralateral femur of every animal was also harvested and frozen for future studies.

RNA Extraction

Femur samples were removed from storage in -80° C freezer and placed into liquid nitrogen. The bone was placed in a 2 mL tube pre-filled with 0.75 ml Qiazol Lysis Reagent® than snap frozen in the liquid nitrogen for approximately 15 seconds. The tube was removed and one 2mm stainless steel bead was added and placed into the Qiagen Tissue Lyser II® for lysing. The bone was lysed for two minutes at 30 Hz and carefully monitored as to not lyse if the sample had thawed. If the sample had thawed or not completely homogenized, the sample was placed back into the liquid nitrogen and the process was repeated. Once the sample was homogenized, the resulting solution was removed and added to a tube containing 1 mL of the Qiazol Lysis Reagent® and placed on ice for at least two minutes. Once all samples had been lysed, 200 µl of chloroform was added, subsequently vortexed, and then allowed to sit on ice for two minutes. Next, each sample was re-vortexed and then centrifuged at 14000 RPM at 4° C for 15 minutes. The aqueous phase was transferred to a new, RNase free, 1.5 ml tube and an equal

volume of isopropanol was added. The tube was inverted several times until the liquid cleared and centrifuged again at 14000 RPM and 4° C for 30 minutes. The supernatant was removed and washed with 500 µl of 70% ethanol and centrifuged at 14000 RPM and 4° C for 5 minutes – this process was repeated once more and the ethanol was removed. The 1.5 ml tube was inverted on a sterile chem-wipe and left to dry the RNA containing pellet. The pellet was then dissolved in 35 µl of RNase-free water and stored at -80° C. The RNA was tested for quality via electrophoresis on a 2% agarose gel performed at 100V for approximately 40 minutes. Additionally, the concentration was determined by adding one µL of the diluted RNA to 99 µl of 10 mM Tris buffer and placed into a UV/Vis Spectrophotometer (Beckman Coutler DU 350). Absorbance values at 260 nm were recorded.

Reverse Transcription and qPCR Quantification

Diluted RNA from each sample was thawed on ice and a total of 2 µg was increased to a volume of 10.4 µl with RNase-free water contained in a 0.2 ml PCR tube. The reverse transcriptase reaction utilized a mixture of following reagents per sample

from the Taqman Reverse Transcription Kit®: $MgCl_2$ (6.61 µl), dNTP Mix (6.0 µl), 10X RT Buffer (3.0 µl), and Random Hexamers (1.5 µl). The reverse transcriptase enzymes RNase Inhibitor (0.6 µl) and Reverse Trancriptase (1.89 µl) were added to the reagent mixture. The 19.6 µl of the reverse transcription polymerase chain reaction reagents and enzymes were added to the 10.4 µl of RNA for a total of 30 µl and gently mixed. The tubes were then placed in a thermal cycler (Eppendorf Mastercycler ®) to run the PCR cycle as follows: 25° C for 10 minutes, 37° C for 60 minutes, 95° C for 5 minutes, and held at 4° C. The subsequent complementary DNA (cDNA) samples were then diluted 1:50 in RNase-free water and stored at -20° C until use for qPCR.

Quantitative real-time polymerase chain reaction (qPCR) was performed to amplify DNA primers of interest. Per each polymerase chain reaction, 9 µl of the diluted cDNA was added to 10 µl of Universal PCR Master Mix (Applied Biosystems ®) and 1 µl of the particular primer set. A 96 well plate was used to house each reaction and covered with a clear adhesive film, paying careful attention to flatten the film to the well's surface. The plate was placed into the centrifuge and gently spun down at 1500

rpm for 2 minutes to mix each sample and eliminate bubbles. The quantitative Real-Time polymerase chain reaction (qRT-PCR) was performed using an ABI 7700 Sequence Detector® (Applied Biosystems) and set up as follows: 50˚C for 2 minutes, 95˚C for 10 minutes, 95˚C for 15 seconds, 60˚C for 1 minute and run for 40 cycles. Samples were run in duplicate and normalized to 18s rRNA. The fold change in expression was normalized to samples from non-fractured, like-strain mice.

Statistical Methods

Statistical analysis was performed using Microsoft Excel 2008. Mean values for qPCR data was computed along with standard deviation. Graphs were generated for mRNA expression of selected genes, including standard deviation bars.

RESULTS

Radiographic Evaluation

Qualitative analysis of radiographs taken post-mortem, before harvest, exhibit that daily subcutaneous PTH treatment increases the size of the fracture callus in C3, AJ, and B6 mice. In all radiographic images, the distal end of the femur is located at the lower left corner of the image.

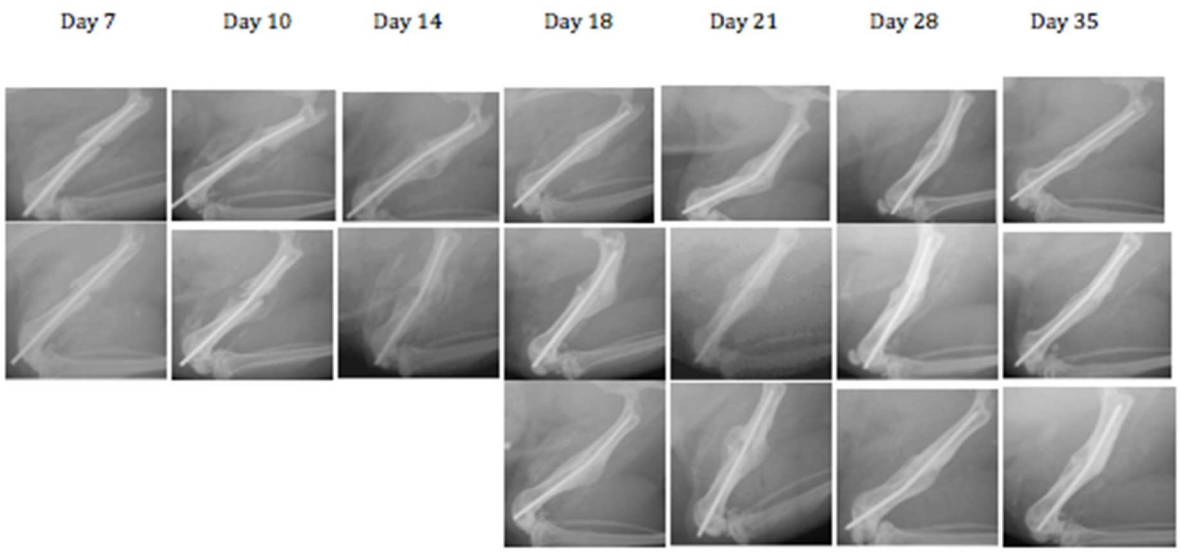

Figure 6. AJ Radiographs. Callus fracture temporal progression from post fracture day 7 to day 35. **Top Row:** Control. **Middle Row:** PTH Treatment Group 1. **Bottom Row:** PTH Treatment Group 2.

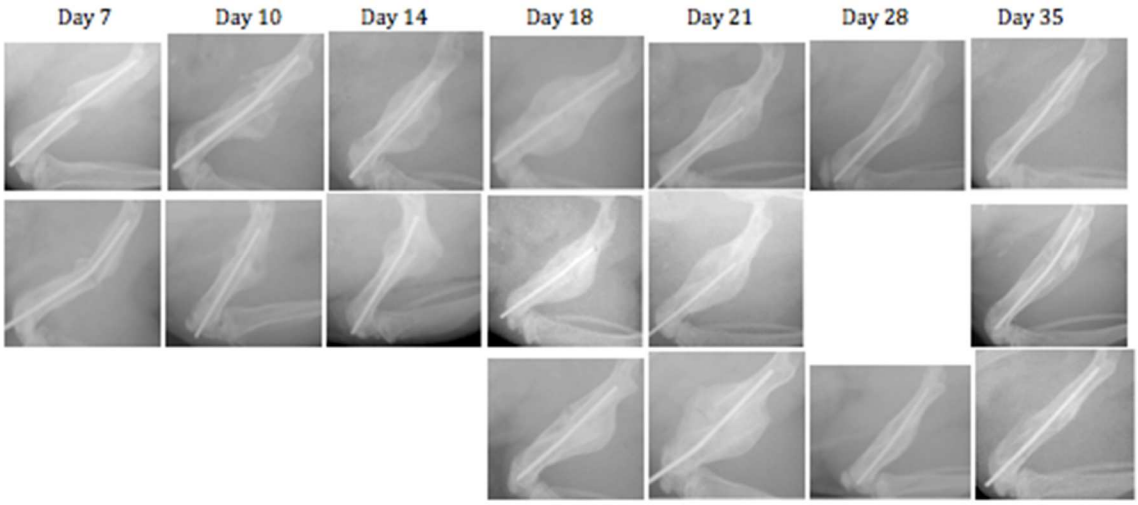

Figure 7. B6 Radiographs. Callus fracture temporal progression from post fracture day 7 to day 35**. Top Row:** Control**. Middle Row:** PTH Treatment Group 1. **Bottom Row:** PTH Treatment Group 2. Omitted picture damaged -- excluded.

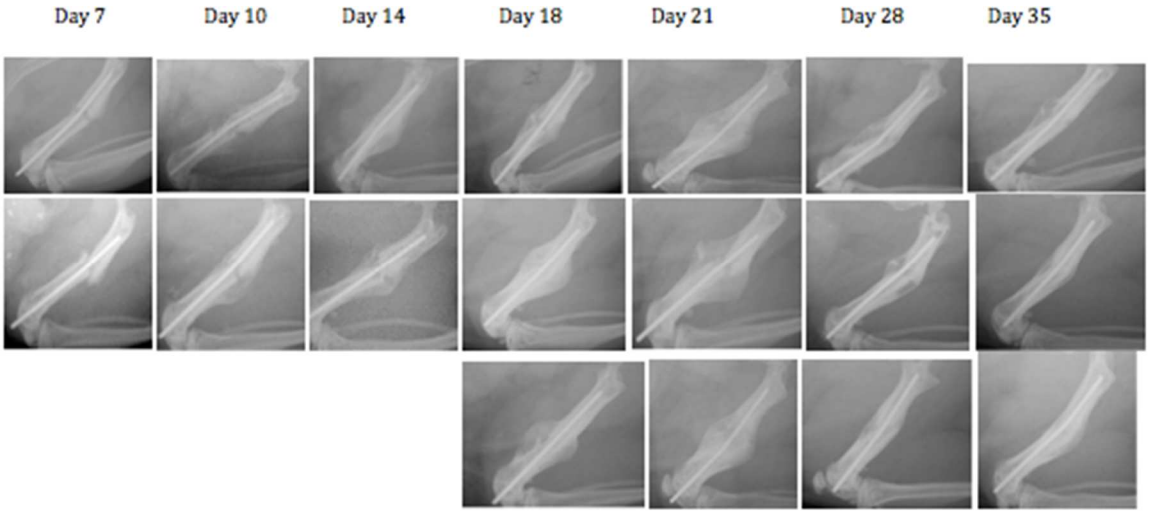

Figure 8. C3 Radiographs. Callus fracture temporal progression from post fracture day 7 to day 35**. Top Row:** Control**. Middle Row:** PTH Treatment Group 1. **Bottom Row:** PTH Treatment Group 2.

The temporal progression from the initial fracture through the period of endochondral formation followed by resorption of the callus and then secondary bone formation with coupled remodeling is easily visualized radiographically (Gerstenfeld et al., 2003). The endochondral callus first appears at day 7, post fracture and reaches maximum size at post fracture day 21. The radiographs suggest that each strain undergoes callus formation, although B6 mice consistently show the largest callus formation and AJ the smallest. Additionally all strains demonstrated cartilage resorption and bone remodeling and it was apparent at time of harvest that PTH treated animals had denser bone. Interestingly either time of treatment resulted in an overall increased bone density by the end of the experimental period that was assessed.

qPCR Analysis

Gene expression for both osteogenic and chondrogenic genes were used to follow the progression of fracture repair. The chondrogenic genes associated with cartilage

formation and analyzed for this study in the order of the progression of their expression were as follows: transcription factor SOX 9, collagen type II alpha 1 (COL2A1), aggrecan (ACAN), and collagen type X alpha 1 (COL10A1). The aggrecan gene is known for its role in the production of large proteoglycan, a structural component of cartilage (Doege, Sasaki, & Yamada, 1991). COL10A1 is responsible for the production of type X collage, which is expressed in hypertrophic chondrocytes during endochondral ossification and COL2A1 is responsible for the production of type II collage, found primarily in cartilage (Gerstenfeld et al., 2006). Finally, SOX9 is expressed in all chondroprogenitor cells and differentiated chondrocytes and thus controls the progression and initiation of chondrogenesis (Mori-Akiyama et al., 2003). Figure 9 shows the relative fold change compared to day 0. Gene expression profiles are presented in temporal order of the progression of chondrocyte differentiation and initiation of ossification. A comparison of these data showed that all three strains showed varying and unique responses to PTH. Within the B6 and AJ strains PTH lead to an earlier commitment to chondrogenesis based on Sox9 expression. Within the B6 strain, PTH induced the most

dramatic overall increase in chondrogenesis and shifted the period of hypotrophy to a slightly earlier period; however, both effects did not appear to prolong the overall period of chondrogenesis. In contrast, in the AJ strain the hypertrophic period was prolonged. On the other hand, PTH did not seem too promote either an earlier or greater amount chondrogenesis in C3 strain but broadened the overall period of hypertrophy increasing Col10a1 to an earlier time and extending its expression to a later period as well.

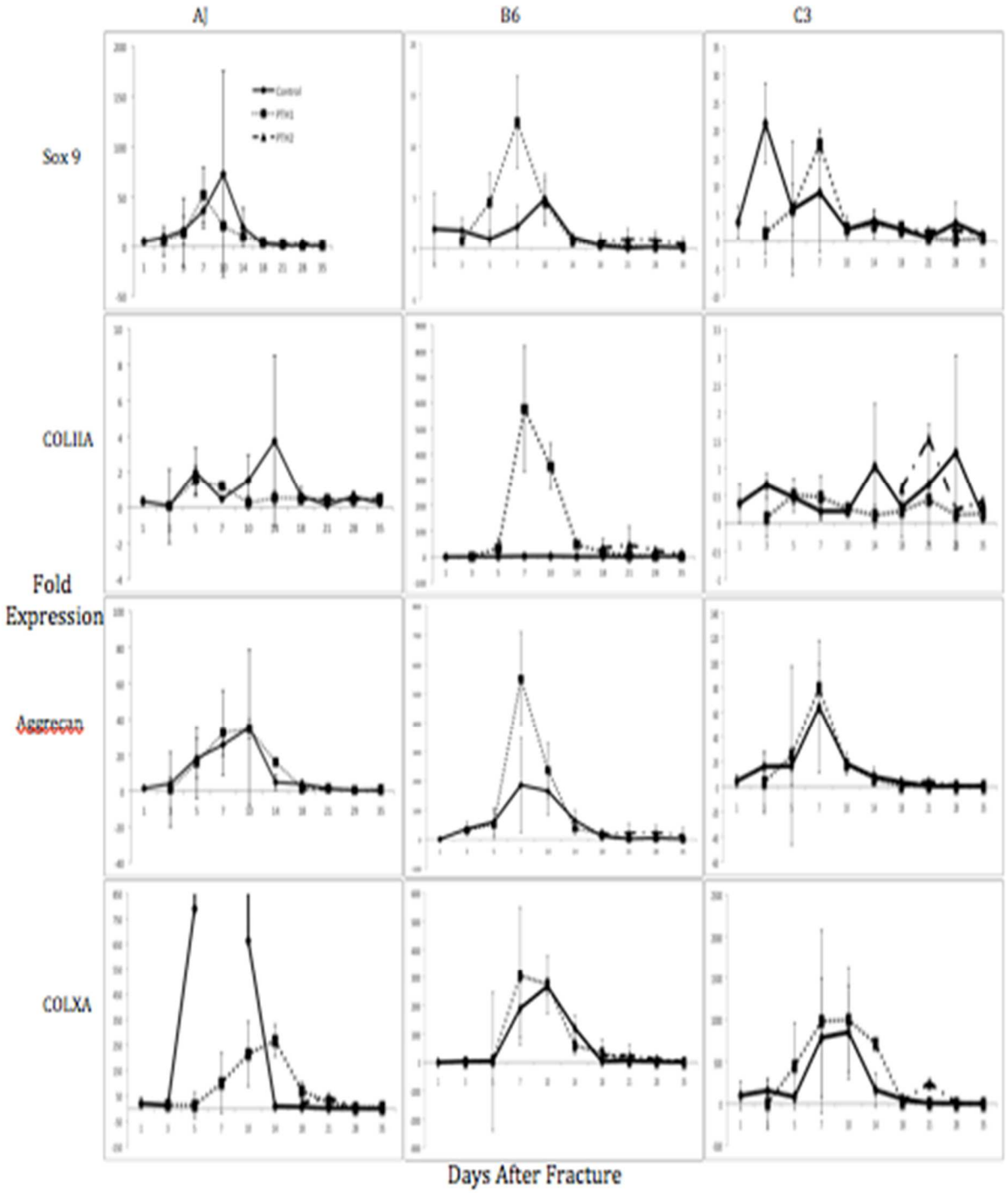

Figure 9. qPCR Analysis of Chondrogenesis. These graphs show the temporal gene expression profiles of known chondrogenic genes of strain AJ, B6, and C3 mice in order of when they are expressed. The x axis shows days post fracture and the y axis is the fold expression compared to the control non-fractured femur. Error bars denote standard deviation. The control mice, PTH-1 treatment group, and PTH-2 treatment group are shown with solid lines, dotted lines, and dashed lines respectively.

Osteogenic genes evaluated include: transcription factor osterix, dentin matrix acidic phosphoprotein 1 (DMP1), osteocalcin, and bone sialoprotein (BSP). Osterix plays a vital role in the maturation of mesenchymal stem cells to osteoblasts (Zhang et al., 2011). DMP1 signals the production of the extracellular matrix and its mineralization from corresponding osteoblasts (Narayanan et al., 2003). Additionally, osteocalcin aids in the development of bone mineralization and calcium homeostasis. Lastly, BSP encodes for a major structural protein of the bone matrix, including mineralized tissues like bone and dentin (Pesesse et al., 2014). Figure 10 shows the relative fold change in expression of the genes known to be involved in osteogenesis.

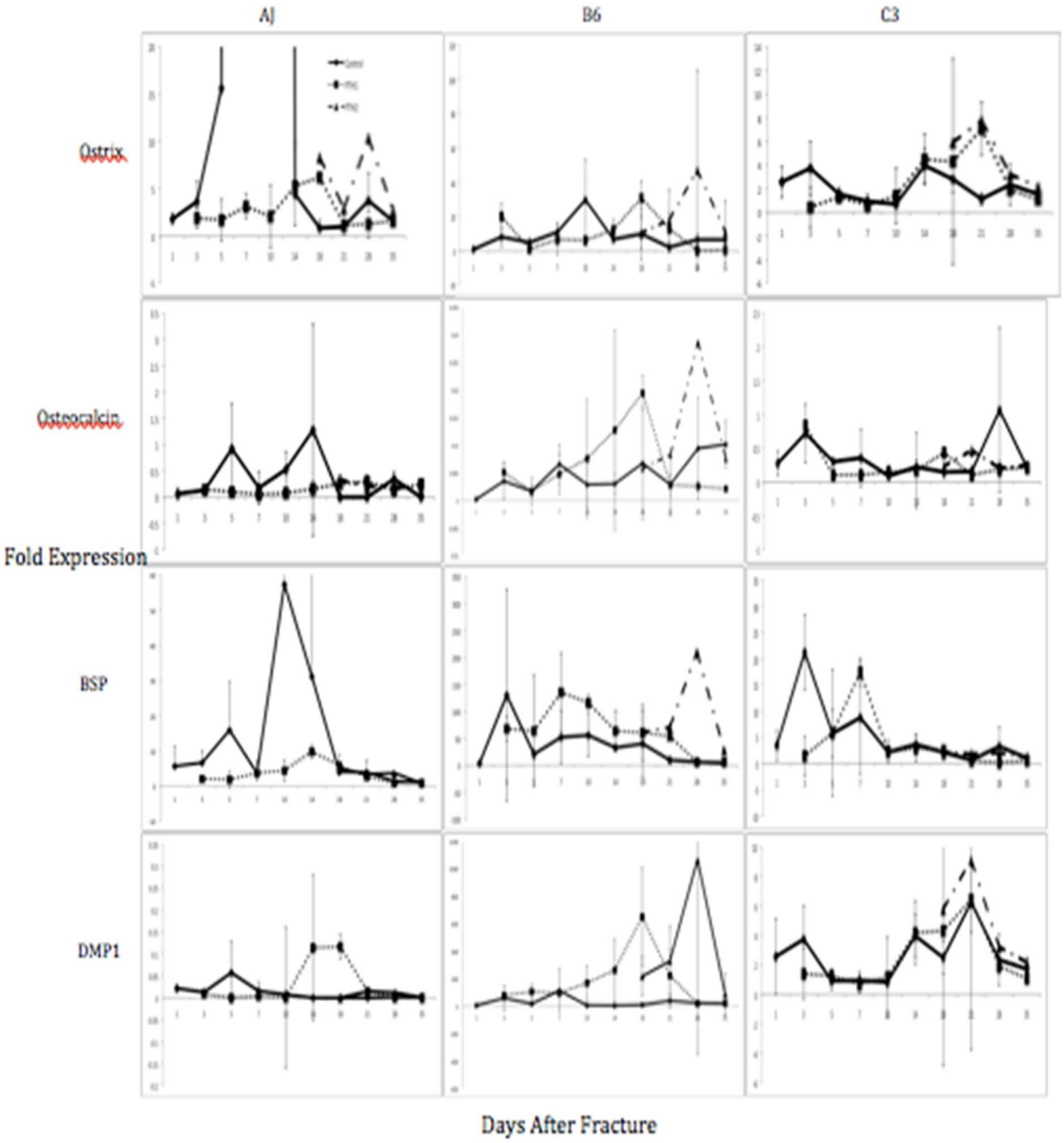

Figure 10. qPCR analysis of Osteogenesis. These graphs show the temporal gene expression profiles of known osteogenic genes of strain AJ, B6, and C3 mice in order of when they are expressed in endochondral bone formation. The x axis shows days post fracture and the y axis is the fold expression compared the control non-fractured femur. Errors bars denote standard deviation. The control mice, PTH-1 treatment group, and PTH-2 treatment group are shown with solid lines, dotted lines, and dashed lines respectively.

Like the chondrogenic genes, these also showed individual effects per strain to PTH. Osterix showed the most consistent response to PTH treatment across all the strains showing that both treatment periods increased its expression at later times during primary and secondary bone formation. Surprisingly in the AJ strain all but DMP1 showed deceased expression and DMP1 was also consistently upregulated for both PTH treatment periods during primary and secondary periods of formations. Once again the B6 strain also showed the greatest quantitative response to the PTH with all of the genes that were examined showing increased levels of expression. Interestingly in the C3 strain osteocalcin showed no overall response to PTH treatment.

DISCUSSION

Study Findings

PTH mediated fracture repair has been shown to be associated with enhanced chondrocyte recruitment and early development of a fracture callus (Kakar et al., 2007). Additionally, it has been shown that different strains of mice have varying osteogenic and chondrogenic gene expression affecting the rate of fracture healing (Jepsen, 2008). The aims of this study, therefore, was to determine how the two time frames of PTH treatment effect fracture healing in different strains of common laboratory mice.

We found that chondrogenic gene expression varies between different strains of mice. In B6 mice, chondrogenic gene expression in the early PTH treatment group was enhanced as compared to the controls. The late PTH treatment group was negligibly affected. In AJ mice, mRNA profiles in the early PTH treatment window showed an earliar and less robust expression compared to the control mice excluding COLXa, which was slightly delayed. In C3 mice, Sox9 expression in the early PTH treatment group was

delayed compared to the control; however, all other gene expression of the early PTH treatment group versus the control mice showed similar expression. Interestingly, the late PTH treatment group had increased COLIIa expression in C3 mice, but seemed unaffected in all other gene expression profiles. Examinations of the chondrogenic mRNA expression profiles show chondrogenesis begins approximately one week post fracture.

The osteogenic gene expression was similar across all strains of mice. In the AJ mice, early PTH treatment down-regulated and delayed the expression of ostrix, osteocalcin, and BSP. Treatment with early PTH delayed and up-regulated DMP1 expression compared to control. Treatment with late PTH only affected ostrix expression, which was upregulated compared to both the control and early PTH group.

In B6 mice, early PTH treatment down-regulated and delayed expression of ostrix but upregulated expression of osteocalcin, BSP, and DMP1, albeit delayed. The late PTH treatment group mRNA expression were greatly enhanced in all genes analyzed.

In C3 mice, the early PTH treatment showed a delayed in the onset of osteogenic gene expression compared to control; however, osteocalcin and DMP1 displayed minimal differences between groups. The late PTH treatment group was upregulated compared to early PTH and control groups. Examination of mRNA expression profiles show the onset of osteogensis begins earliest in AJ mice at approximately day 10 post fracture.

Taken together with radiographic analysis, this data supports previous studies that demonstrate the bone remodeling enhancing effect of PTH on chondrogensis. In addition, PTH seems to have a significant effect on the initiation of osteogenesis and the strength of mRNA expression in genes associated with endochondral bone formation. This study also is consistent with previous studies regarding genetic differences in murine fracture models. C3 mice demonstrate the less robust mRNA expression of examined genes and the latest period of osteogenesis and AJ are the most affected by PTH treatment.

Future Considerations

Fracture healing is a complex genetic trait with both genetic and environmental factors contributing to phenotypic properties. Individuals with genetically different backgrounds therefore may elicit different responses to similar skeletal stress. Employing different environmental perturbations in further studies, such as phosphate restriction to inhibit healing, could be utilized to further understand the element that regulate fracture healing. This study provides the first findings that suggest that the effect of PTH treatment will be variability regulated by the genetic background in differing strains of mice with highly variable bone qualities. Serum collected from each mouse during the terminal bleeds should be evaluated to assess if this variation is systemically reflected in variations in mineral metabolism. In addition both mechanical and structural testing needs to be done on both fractured and contralateral femurs in PTH treated and control mice to determine how PTH effects the phenotypic properties of both fracture healing and bone mineral density and twist to break points for each time point. This would go further in demonstrating the potential use of PTH as a pharmacologic agent for fracture

healing. Finally histological preparations of the callus tissues using selective staining for both cartilage and mesenchymal tissues would help determine the definitive nature of how skeletal stem cells are directed towards endochondral tissue development in response to PTH.

REFERENCES

Beamer, W.G., Donahue, L.R., Rosen, C.J., & Baylink, D.J. (1996, May). Genetic Variability in Adult Bone Density Among Inbred Strains of Mice. Elsevier Bone Vol. 18 No. 5 297-403.

Della Rocca, G. J., Crist, B. D., Murtha, Y. M. (2010). Parathyroid hormone: Is there a Role in Fracture Healing. *Journal of Orthopaedic Trauma, 24(S),* 31-35 .

Dimitriou, R., Carr, I. M., West, R. M., Markham, A. F., & Giannoudis, P. V. (2011). Genetic predisposition to fracture non-union: a case control study of a preliminary single nucleotide polymorphisms analysis of the BMP pathway. *BMC Musculoskeletal Disorders*, *12*, 44.

Doege, K. J., Sasaki, M., Kimura, T., & Yamada, Y. (1991). Complete coding sequence and deduced primary structure of the human cartilage large aggregating proteoglycan, aggrecan. Human-specific repeats, and additional alternatively spliced forms. *Journal of Biological Chemistry, 266(2).* 894-902.

Einhorn, T. A. (1995). Enhancement of fracture-healing. *The Journal of bone and joint surgery. American volume, 77(6),* 940–956.

Einhorn, T. A. (1998). The cell and molecular biology of fracture healing. *Clinical Orthopaedics and Related Research*, (355 Suppl), S7–21.

Ellegaard, M., Jorgensen, N. R., Schwarz, P.(2010). Parathyroid hormone and bone healing. *Calcif Tissue Int, 87(1),* 1-13.

Gerstenfeld, L. C., Cullinane, D. M., Barnes, G. L., Graves, D. T., & Einhorn, T. A. (2003). Fracture healing as a post-natal developmental process: Molecular, spatial, and temporal aspects of its regulation. *Journal of Cellular Biochemistry*, *88*(5), 873–884.

Gerstenfeld, L. C., Alkhiary, Y. M., Krall, E. A., Nicholls, F. H., Stapleton, S. N., Fitch, J. L., … Einhorn, T. A. (2006). Three-dimensional Reconstruction of Fracture Callus Morphogenesis. *Journal of Histochemistry & Cytochemistry*, *54*(11), 1215–1228.

Jepsen, K. J., Price, C., Silkman, L. J., Nicholls, F. H., Nasser, P., Hu, B., … Gerstenfeld, L. C. (2008). Genetic variation in the patterns of skeletal progenitor cell differentiation and progression during endochondral bone

formation affects the rate of fracture healing. *Journal of Bone and Mineral Research: The Official Journal of the American Society for Bone and Mineral Research*, *23*(8), 1204–1216.

Kakar, S., Einhorn, T. A., Vora, S., Mirara, L. J., Hon, G., Wigner, N. A., Toben, D., Jacobsen, K. A., Al-Sebaei, M. O., Song, M., Trackman, P. C., Morgan, E. F., Gerstenfeld, L. C., & Barnes, G. L. (2007). Enhanced chondrogenesis and wnt signaliing in PTH-treated fractures. *Journal of Bone and Mineral Research, 22(12),* 1903-1910.

Karsenty, G. (2008). Transcriptional control of skeletogenesis. *Annual Review of Genomics and Human Genetics*, *9*, 183–196.

Marturano, J. E., Cleveland, B. C., Byrne, M. A., O'Connell, S. L., Wixted, J. J., & Billiar, K. L. (2008). An improved murine femur fracture device for bone healing studies. *Journal of Biomechanics*, *41*(6), 1222–1228.

Mori-Akiyama, Y., Akiyama, H., Rowitch, D. H., & Crombrugghe, B. de. (2003). Sox9 is required for determination of the chondrogenic cell lineage in the cranial neural crest. *Proceedings of the National Academy of Sciences*, *100*(16), 9360–9365.

Neer, R. M., Arnaud, C. D., Zanchetta, J. R., Prince, R., Gaich, G. A., Reginster, J. Y., Hodsman, A. B., Eriksen, E. F., Ish-shalom, S., Genant, H. K., Wang, O., Mtlak, B. H. (2001). Effect of parathyroid hormone (1-34) on fractures and bone mineral density in postmenopausal women with osteoporosis. *New England Journal of Medicine, 344,* 1434-1441.

Pesesse, L., Sanchez, C., Walsh, D. A., Delcour, J. P., Baudouin, C., Msika, P., Henrotin, Y. (2014). Bone sialoprotein as a potential key factor implicated in the pathophysiology of osteoarthritis. *Osteoarthritis Cartilage, 22(4),* 547-56.

Poole, K., Reeve, J. (2005). Parathyroid hormone – a bone anabolic and catabolic agent. *Curr Opin Pharmacol, 5(6),* 617-617.

Ross, M. H., & Pawlina, W. (2010). *Histology: A Text and Atlas (Histology* (6th ed.). Lippincott Williams & Wilkins.

Sims, N. A., Dupont, S., Krust, A., Clement-Lacroix, P., Minet, D., Resche-Rigon, M., … Baron, R. (2002). Deletion of estrogen receptors reveals a regulatory role for estrogen receptors-beta in bone remodeling in females but not in males. *Bone*, *30*(1), 18–25.

Strohbach, C. A., Strong, D. D., Rundle, C. H. (2011). Gene therapy applications for Fracture repair. *Gene Therapy Applications.* ISBN: 9789533075419, InTech.

Vaughn, D. W. (2008) Bone histogenesis. *Medical histology syllabus* (p7-12). Boston University School of Medicine. Department of Anatomy and Neurobiology.

Zhang, C., Tang, W., Li, Y., Yang, F., Dowd, D. R., & Macdonald, P. N. (2011). Osteoblast-specific transcription factor Osterix increases Vitamin D receptor gene expression in Osteoblasts. *Public Library of Sciences ONE Journal. 6(10),* e26504.

CURRICULUM VITAE